

Interaction of Nonstructural Protein 5A of the Hepatitis C Virus with Src Homology 3 Domains Using Noncanonical Binding Sites

Melanie Schwarten,^{†,‡,§,||} Zsófia Sólyom,^{†,‡,§} Sophie Feuerstein,^{†,‡,§} Amine Aladağ,^{||,⊥} Silke Hoffmann,^{||} Dieter Willbold,^{‡,||,⊥} and Bernhard Brutscher^{*,†,‡,§}

[†]Institut de Biologie Structurale, Université Grenoble 1, 41 rue Jules Horowitz, 38027 Grenoble Cedex 1, France

[‡]Commissariat à l'Energie Atomique et aux Energies Alternatives (CEA), Grenoble, France

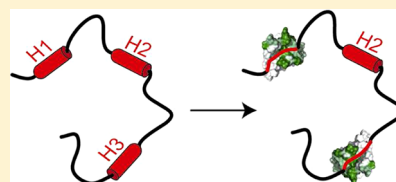
[§]Centre National de Recherche Scientifique (CNRS), Grenoble, France

^{||}Institute of Complex Systems (ICS-6) Structural Biochemistry, Forschungszentrum Jülich, 52425 Jülich, Germany

[⊥]Institut für Physikalische Biologie, Heinrich-Heine-Universität, 40225 Düsseldorf, Germany

S Supporting Information

ABSTRACT: Src homology 3 (SH3) domains are widely known for their ability to interact with other proteins using the canonical PxxP binding motif. Besides those well-characterized interaction modes, there is an increasing number of SH3 domain-containing complexes that lack this motif. Here we characterize the interaction of SH3 domains, in particular the Bin1-SH3 domain, with the intrinsically disordered part of nonstructural protein 5A of the hepatitis C virus using noncanonical binding sites in addition to its PxxP motif. These binding regions partially overlap with regions that have previously been identified as having an increased propensity to form α -helices. Remarkably, upon interaction with the Bin1-SH3 domain, the α -helical propensity decreases and a fuzzy complex is formed.



Src homology 3 domains (SH3 domains) are small, 50–80-residue protein domains that mediate protein–protein interactions. They can be found in a variety of proteins regulating dynamic cellular processes like signal transduction. Their structure is characterized by a five-stranded β -barrel with a hydrophobic cleft on the surface (Figure 1A), which is mainly formed by aromatic residues. The hydrophobic pocket recognizes left-handed polyproline type II (PPII) helices. This proline-rich sequence motif, called the PxxP motif, can interact in two orientations with the SH3 domain and can thus be classified into two distinct groups. Class I ligands have the consensus sequence +pxPxxP in common (P, conserved proline residue; p, often proline residue; +, positively charged amino acid residue; x, any amino acid residue), whereas class II ligands consist of a PxxPp+ sequence. The basic amino acid residue interacts with a negatively charged residue in the RT loop of the SH3 domain and thus defines the orientation of the ligand (for a review, see ref 1).

In addition to this canonical PxxP binding mode, SH3 domains also interact with protein partners via other, noncanonical binding modes. An increasing number of complexes between SH3 domains and peptides that lack the canonical PxxP motif have been identified and structurally characterized.² These nonconsensus SH3 ligands can be very diverse, ranging from the SAMP motif that interacts with the SH3 domain of DDEF1 (development- and differentiation-enhancing factor 1)³ to the PxxDY motif that interacts with Eps8L1⁴ and a (R/K)xx(R/K) motif that binds to the Gads-SH3 domain.^{5,6} Recently, Perez et al.⁷ reported an allosteric mechanism for the SH3 domain of c-Src that interacts via a

noncanonical binding mode with its Unique domain. This interaction is prevented when a polyproline ligand is bound to the canonical PxxP binding site at the opposite surface of the SH3 domain.⁷ Another motif containing mainly positively charged amino acid residues was reported to bind to the SH3 domain of bridging integrator protein 1 (Bin1),⁸ a proapoptotic tumor suppressor, which is the major target of this study. Via its SH3 domain, Bin1 interacts with a variety of other proteins, including c-Myc and dynamin.^{9,10} Furthermore, interactions of the Bin1-SH3 domain with viral proteins, including nonstructural protein 3 of alphaviruses¹¹ and nonstructural protein 5A (NSSA) of the hepatitis C virus, have been reported.^{12–14}

Nonstructural protein 5A (NSSA) of the hepatitis C virus (HCV) is involved in a variety of viral and cellular processes. NSSA is indispensable for viral replication and particle assembly, although no direct enzymatic activity has been attributed to it. The domain structure of NSSA is shown in Figure 2A. Its N-terminal region contains an amphipathic helix, anchoring NSSA to the membranes of the endoplasmic reticulum, followed by a well-folded zinc-binding domain (D1).^{15,16} The C-terminal part of NSSA, comprising domains D2 and D3, is intrinsically disordered.^{17–19} The three domains are linked by so-called low-complexity sequences LCS-1 and LCS-2. LCS-2 contains a proline-rich region comprising two class II PxxP motifs (PP2.1 and PP2.2) as well as a class I motif

Received: March 21, 2013

Revised: July 12, 2013

Published: August 15, 2013

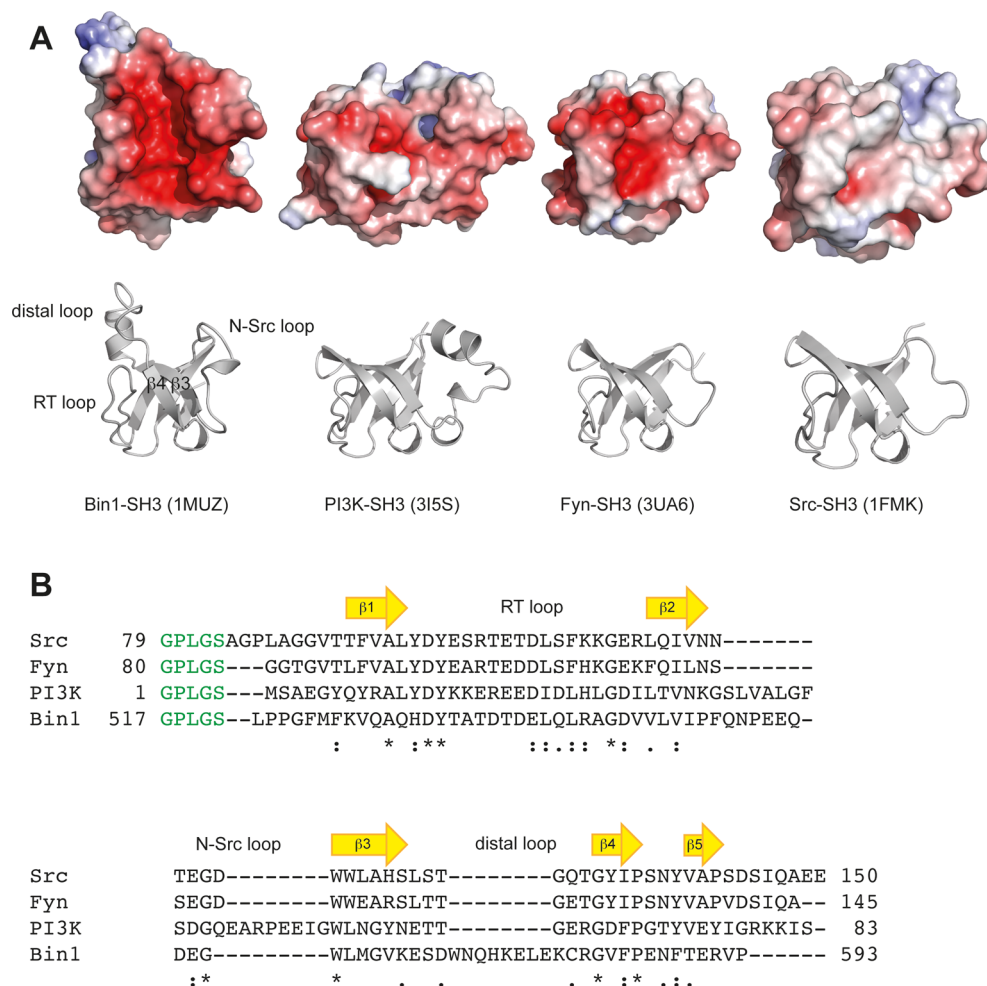


Figure 1. (A) Structures and electrostatic surface potentials of SH3 domains of Src, Fyn, PI3K, and Bin1 used in this study. Surface electrostatic potentials of the Bin1-SH3 [Protein Data Bank (PDB) entry 1MUZ], PI3K-SH3 (PDB entry 3I5S), Fyn-SH3 (PDB entry 3UA6), and Src-SH3 (PDB entry 1FMK) domains were calculated using the APBS tools⁴⁷ implemented in PyMOL.⁴⁸ (B) Sequence alignment of the different SH3 domains. Positions of the β -strands and the loop regions are indicated at the top. The five N-terminal amino acid residues that do not belong to the SH3 domain but result from cloning and PreScission cleavage are colored green.

(PP1.2). It has been shown that the PP2.2 motif is highly conserved among different HCV genotypes and can interact with a variety of SH3 domains of the Src kinase family, including Fyn, Lyn, Lck, and Hck, as well as the SH3 domains of the adaptor proteins Grb2 and Bin1.^{20,21} Here we report on the results of a nuclear magnetic resonance (NMR) investigation of the interaction of NSSA with the SH3 domains of Bin1, PI3K, Fyn, and Src (Figure 1B). Our results reveal that in addition to the canonical SH3 binding to the PxxP motif, NSSA has two additional low-affinity binding sites for noncanonical SH3 binding. These noncanonical modes of binding between NSSA and the Bin1-SH3 domain have been further investigated in terms of structure and conformational dynamics.

MATERIALS AND METHODS

Protein Production and Purification. The NSSA fragment containing residues 191–369 [NSSA(191–369)] was expressed and purified as previously described.²² A second NSSA fragment, NSSA(191–340), is a shorter variant of NSSA(191–369) featuring a deletion of the second LCS that contains the canonical SH3 binding motifs (see Figure 1B). It was generated by polymerase chain reaction (PCR) using

NSSA(191–369) as a template with 5'-GGAGGAGGATCC-CTCCGCGCGCGGTGAACCGGAACC-3' and 5'-GGAGGAGCGGCGCGCTTAATGCACCACCGCGGCACATAATC-3' as primers. The PCR product was subcloned into pGex-6P-2 using BamHI and NotI restriction sites. Expression and prepurification of NSSA(191–340) were conducted as described for NSSA(191–369), whereas the PreScission cleavage products were subjected to a second glutathione-Sepharose 4B affinity chromatography (GE Healthcare) step, followed by size exclusion chromatography [HighLoad SD75 16/60 (GE Healthcare)]. SH3 domains were expressed as GST fusion proteins and purified as previously described.^{17,23–25} A sequence alignment of these SH3 domains is shown in Figure 1B.

NMR Spectroscopy. NMR experiments were performed on Agilent VNMRs 600 and 800 MHz spectrometers equipped with cryogenically cooled triple-resonance (HCN) probes with pulsed z-field gradients. All NMR data were processed using NMRPipe²⁶ and evaluated using CcpNMR.²⁷

The interactions of NSSA(191–369) with the Src-, Fyn-, PI3K-, and Bin1-SH3 domains were studied as reported previously.¹⁷ Briefly, increasing amounts of an unlabeled SH3 domain (1.0 mM stock solution) were added to [¹³C;

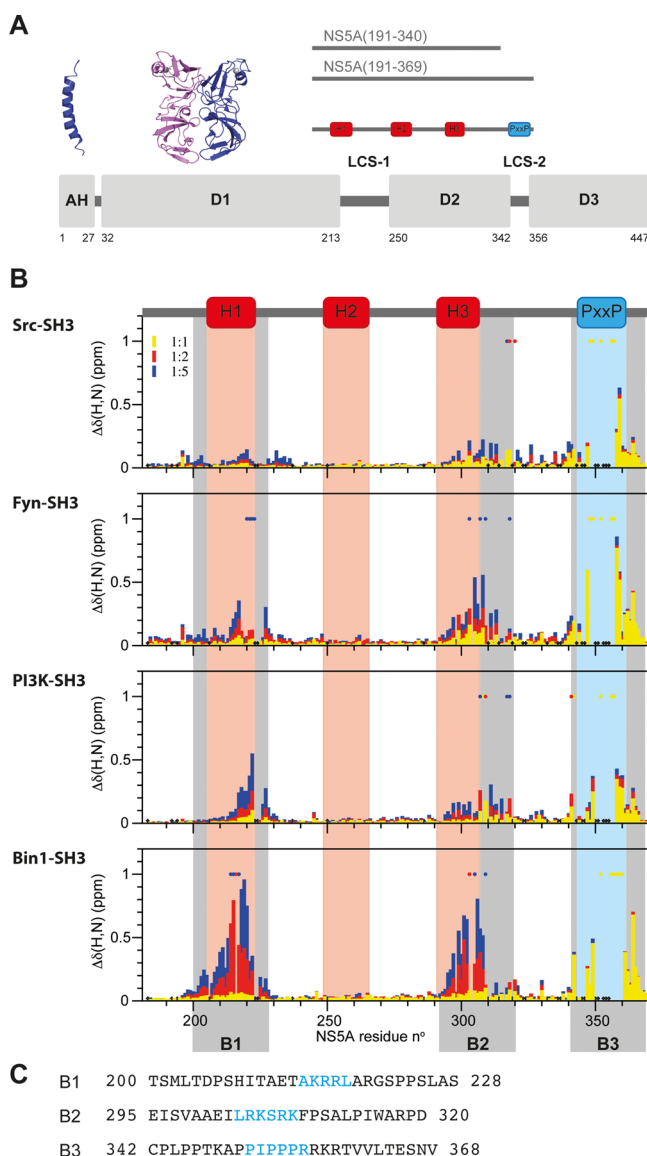


Figure 2. (A) Schematic representation of the domain organization of NSSA. Ribbon representations of the N-terminal amphipathic helix (AH, blue, PDB entry 1R7E) and dimeric globular domain 1 (D1, pink and blue, PDB entry 3FQM) are shown. Red and blue bars indicate the location of the transiently populated α -helices and the PxxP motifs, respectively. (B) Chemical shift perturbations in NSSA(191–369) upon titration with the SH3 domains of Src, Fyn, PI3K, and Bin1 are mapped on the primary sequence. On top of the histograms, the locations of the transiently formed α -helices and the PxxP motifs are shown. For a NSSA:SH3 ratio of 1:1 (yellow), chemical shift changes can mainly be detected close to the PxxP motifs. Chemical shift perturbations at ratios of 1:2 and 1:5 are colored red and blue, respectively. Residues for which no signal could be detected due to line broadening upon interaction are marked with yellow circles for the 1:1 ratio and red and blue circles for the 1:2 and 1:5 ratios, respectively. Proline residues are represented by black diamonds. (C) Amino acid sequences of the binding regions.

U- ^{15}N]-NSSA(191–369) (starting concentration of 0.1 mM), and two-dimensional (2D) ^1H - ^{15}N BEST-TROSY²⁸ spectra were recorded at [NSSA(191–369)]:[Bin1-SH3] molar ratios of 1:0, 1:0.5, 1:1, 1:2, and 1:5 at 5 °C. To identify the binding interfaces of NSSA(191–340) and Bin1-SH3, chemical shift changes upon addition of Bin1-SH3 to NSSA(191–340) were mapped. Experiments were conducted in a single titration series

by adding increasing amounts of U- ^{15}N -labeled Bin1-SH3 (1.54 mM stock solution) to [U- ^{13}C ; U- ^{15}N]-NSSA(191–340) (starting concentration of 0.16 mM). 2D BEST-TROSY-HNco experiments,²⁹ which allow the separation of signals belonging to [U- ^{13}C ; U- ^{15}N]-NSSA(191–340) from those belonging to [U- ^{15}N]-NSSA Bin1-SH3, were conducted at 5 °C at [NSSA(191–340)]:[Bin1-SH3] molar ratios of 1:0, 1:0.5, 1:1, 1:2, 1:5, 1:10, and 0:1. The chosen NSSA concentration is close to the solubility limit of NSSA. Therefore, we did not attempt to record Bin1-SH3 spectra in the presence of a large excess of NSSA. The weighted chemical shift changes, $\Delta\delta(\text{H},\text{N})$, were calculated using the following equation: $\Delta\delta(\text{H},\text{N}) = \{[10\Delta\delta(\text{H})]^2 + \Delta\delta(\text{N})^2\}^{1/2}$. The dissociation constants K_d^1 (for binding of SH3 to B1) and K_d^2 (for binding of SH3 to B2) were then estimated by fitting the data to the equations $\Delta\delta_{\text{B1}} = \Delta\delta_{\text{max}}([PL_1] + [PL_1L_2])/[P_0]$ and $\Delta\delta_{\text{B2}} = \Delta\delta_{\text{max}}([PL_2] + [PL_1L_2])/[P_0]$, with the concentrations of free SH3 (L), free NSSA (P), SH3-bound B1 (PL_1), SH3-bound B2 (PL_2), and SH3-bound B1 and B2 (PL_1L_2) given by the equations $[L] = -a/3 + [2(a^2 - 3b)]^{1/2} \cos(\varphi/3)/3$, $[P] = ([P_0]K_d^1K_d^2)/d$, $[PL_1] = ([P_0][L]K_d^2)/d$, $[PL_2] = ([P_0][L]K_d^1)/d$, $[PL_1L_2] = ([P_0][L]^2)/d$, respectively. $[P_0]$ and $[L_0]$ are the total NSSA and SH3 concentrations, respectively, and the parameters a , b , c , d , and φ are given by

$$a = K_d^1 + K_d^2 - [L_0] + 2[P_0]$$

$$b = K_d^1K_d^2 - [L_0]K_d^1 - [L_0]K_d^2 + [P_0]K_d^1 + [P_0]K_d^2$$

$$c = -[L_0]K_d^1K_d^2$$

$$d = K_d^1K_d^2 + [L](K_d^1 + K_d^2) + [L]^2$$

$$\varphi = \arccos(-2a^3 + 9ab - 27c)/[2\sqrt{(a^2 - 3b)^3}]$$

To identify Bin1-SH3 residues affected by either the B1 or B2 binding sites separately, we used the synthetic NSSA peptides NSSA(200–228) and NSSA(295–320), which were purchased as C18 reversed-phase high-performance liquid chromatography-purified products (JPT Peptide Technologies) containing an acetylated N-terminus and an amidated C-terminus. For chemical shift mapping purposes, 2D ^1H - ^{15}N BEST-TROSY spectra of the U- ^{15}N -labeled Bin1-SH3 domain in isolation and in the presence of an approximately 10-fold excess of the individual peptides were recorded.

Carbonyl (CO) and C^α chemical shifts of NSSA(191–340) in the free and complexed state (10-fold excess of Bin1-SH3) were determined using three-dimensional BEST-TROSY HNCO and HNCA experiments.²⁹ Secondary chemical shifts were calculated on the basis of random-coil chemical shifts and corrected for next neighbor effects.^{30,31} Secondary structure propensities were determined with the SSP program using H^N , N , C^α , and CO chemical shifts as input data.³²

^{15}N relaxation experiments for measuring T_1 , T_2 , and heteronuclear $\{^1\text{H}\}$ - ^{15}N NOE (hetNOE) values were performed at a ^1H frequency of 800 MHz for the free and SH3-bound NSSA(191–340) using standard pulse sequences.³³

RESULTS

NSSA Binds to SH3 Domains Using Different Interaction Modes. The interaction of the intrinsically disordered central part of NSSA (residues 191–369) with the

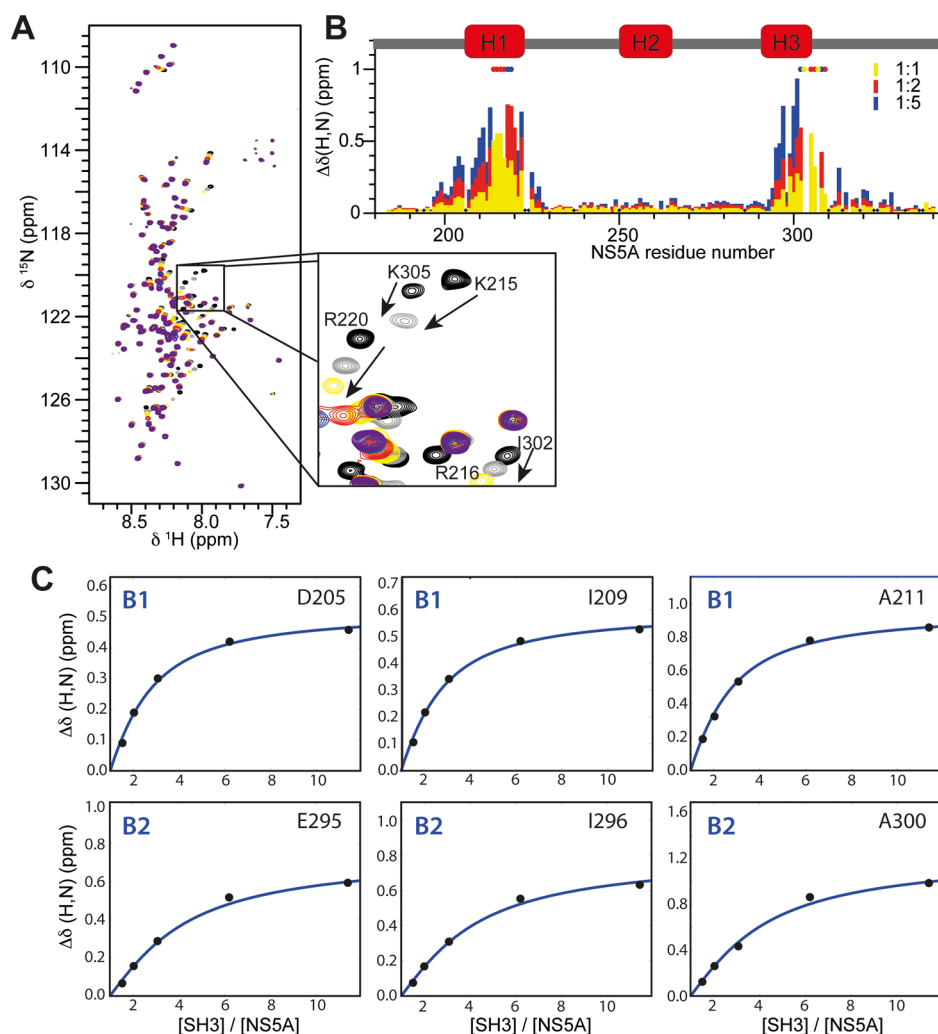


Figure 3. Interaction of NSSA(191–340) with Bin1-SH3. (A) Superposed ^1H - ^{15}N correlation spectra of NSSA(191–340) upon titration with increasing amounts of Bin1-SH3. The different color-coded spectra correspond to [NSSA(191–369)]:[Bin1-SH3] molar ratios of 1:0 (black), 1:0.5 (gray), 1:1 (yellow), 1:2 (red), 1:5 (blue), and 1:10 (purple). (B) Chemical shift perturbations measured at NSSA(191–340):Bin1-SH3 ratios of 1:1, 1:2, and 1:5 are colored yellow, red, and blue, respectively. (C) Binding curves obtained for representative residues in the two binding regions, B1 and B2. A global fit yielded a K_d of $100 \pm 50 \mu\text{M}$ for the B1 region and a K_d of $240 \pm 50 \mu\text{M}$ for the B2 region.

SH3 domains of Src-, Fyn-, and PI3-kinases as well as the Bin1-SH3 domain was mapped using NMR titration experiments in which increasing amounts of SH3 were added to an NSSA sample. All four SH3 domains induced changes in the NMR spectra of NSSA (Figure 2B), thus indicating that NSSA interacts with each of these SH3 domains. First, addition of small amounts of SH3 led to line broadening of several NSSA residues within the PP2.2 motif [namely, I352, R356, and R357 (see Figure 2A)]. In addition, NMR signals from amino acid residues adjacent to the PP2.2 motif showed chemical shift changes during titration. Titration of NSSA with either Src-SH3, Fyn-SH3, or PI3K-SH3 at substoichiometric ratios resulted in a continuous change in the chemical shifts, indicating fast exchange kinetics on the NMR time scale, which is indicative of a comparatively low binding affinity. In contrast, as already reported previously,¹⁷ upon titration with Bin1-SH3, separate NMR signals are detected for the SH3-bound and free states of NSSA, indicating a slow exchange process and comparatively high binding affinity.

Besides the interaction with SH3 domains mediated by a canonical PxxP motif located in the LCS-2 region of NSSA (binding site B3), we were able to identify two additional

peptide regions in NSSA that interact with the four SH3 domains mentioned above (Figure 2B). Upon addition of SH3 at concentrations higher than the equimolar concentration, chemical shift changes were observed for NSSA residues 200–228 (binding site B1) and 295–320 (binding site B2). Interestingly, these binding sites comprise peptide regions that have been shown to transiently adopt α -helical structure.¹⁷ While for the Src-SH3 domain only marginal chemical shift changes in the B1 and B2 regions were observed, possibly indicating a very low binding affinity, large chemical shift changes and broadening of some NMR signals are characteristic of the titration with the Bin1-SH3 domain. For the Fyn-SH3 and PI3K-SH3 domains, an intermediate situation was observed. Upon addition of Fyn-SH3 to NSSA, residues 214–230 showed chemical shift changes and central residues 218–221 experienced line broadening beyond the NMR detection limit at a 1:5 NSSA:SH3 ratio. Similarly, in the second binding region, chemical shift changes are observed for residues 295–320 with several signals disappearing at a 1:5 ratio. For the PI3K-SH3 domain, no severe line broadening was detected in the B1 region, but several signals in the B2 region disappeared upon titration.

Noncanonical SH3 Binding to NSSA. To further investigate the interaction of the SH3 domain with low-affinity NSSA binding sites B1 and B2, we designed a shorter NSSA construct, NSSA(191–340), that lacks the high-affinity SH3 binding site (PxxP motif). The ^1H – ^{15}N correlation spectra of NSSA(191–340) and NSSA(191–369) almost perfectly overlap (Figure S1 of the Supporting Information), indicating that the structural and dynamic characteristics of NSSA are very similar within the two constructs. Importantly, the transient helical structures that have been identified in the longer NSSA(191–369) fragment¹⁷ remain unaltered in NSSA(191–340), making this a suitable protein construct for studying the noncanonical binding of NSSA to SH3 domains. In the following, we will focus on the interaction of NSSA(191–340) with the Bin1-SH3 domain that induces the largest chemical shift changes in the NSSA spectrum. A very similar pattern of chemical shift changes and line broadening was observed in NMR titration experiments (Figure 3B) as shown in Figure 2B for the longer NSSA construct, indicating that the observed perturbation is due to direct SH3 binding events, and not to conformational changes induced by the high-affinity interaction of the SH3 domain with the PxxP motif of NSSA. In Figure 3C, the chemical shift changes of representative residues within the two binding regions that do not show significant line broadening are plotted as a function of the SH3:NSSA concentration ratio for the NSSA(191–340) construct. A global fit of the titration curves assuming a kinetic model with two independent binding sites, B1 and B2, yields a K_d^1 of $100 \pm 50 \mu\text{M}$ for the B1 region and a K_d^2 of $240 \pm 50 \mu\text{M}$ for the B2 region. As shown previously for the long NSSA(191–369) construct, the B1 site has a 2–3-fold higher binding affinity for the Bin1-SH3 domain than the B2 site. The absolute K_d values should be taken with care as the NSSA constructs have a tendency to aggregate, and it is therefore difficult to accurately estimate the binding-competent NSSA concentration.

Our titration data also provided information about the Bin1-SH3 residues that are involved in the interaction with the noncanonical low-affinity binding sites of NSSA. The measured ^1H and ^{15}N chemical shift changes are plotted in Figure 4A as a function of the Bin1-SH3 sequence, and in Figure 4B, they are color-coded on the structure of Bin1-SH3. Binding of SH3 to NSSA segments B1 and B2 affects mainly the residues located in the canonical binding pocket of SH3 domains for polypeptide motifs, which is formed by the RT and N-Src loop as well as β -strands 3 and 4. Low- and high-affinity NSSA binding thus affects the same binding pocket on the surface of the SH3 domain. Possible differences in the modes of binding of B1 and B2 to Bin1-SH3 were further investigated by NMR titration experiments of ^{15}N -labeled Bin1-SH3 with the unlabeled synthetic peptides B1(200–228) and B2(295–320). For both peptides, very similar chemical shift changes were obtained as in the case of the NSSA(191–340) construct containing both binding sites (Figure S2 of the Supporting Information).

Our results confirm that each SH3 domain can bind to only a single NSSA interaction site, and that the different binding modes are mutually exclusive as they all compete for the same binding pocket on the SH3 domain.

Changes in the NSSA Structural Ensemble Induced by SH3 Binding. As the two low-affinity binding regions B1 and B2 partly overlap with peptide segments that were previously identified as having increased α -helical propensities, we next investigated how SH3 binding influences the conformational sampling properties of NSSA. ^{13}C secondary chemical shifts are

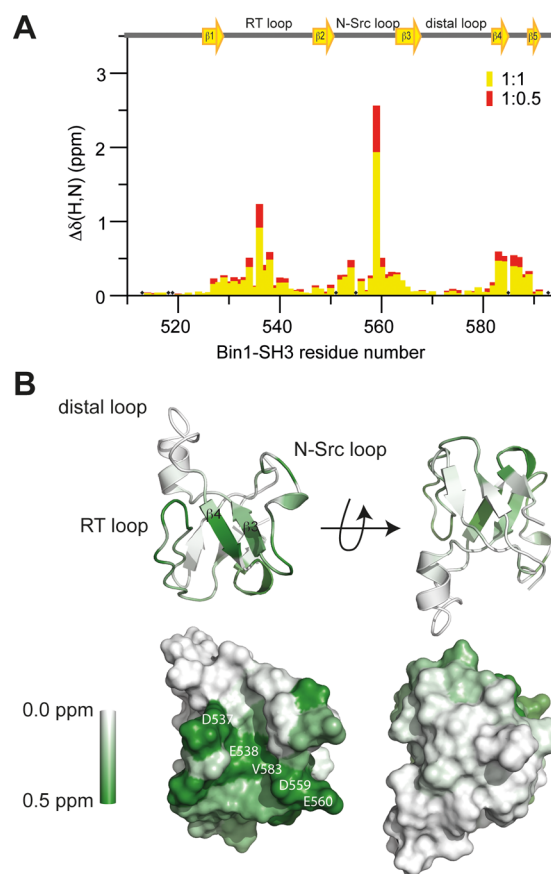


Figure 4. Chemical shift changes observed upon interaction of NSSA(191–340) with Bin1-SH3 plotted as a function of the Bin1-SH3 sequence (A) and mapped onto the Bin1-SH3 structure (B). (A) On top of the histogram, the locations of the β -strands and loop regions are shown. Chemical shift perturbations at NSSA(191–340):Bin1-SH3 ratios of 1:1 and 1:0.5 are colored yellow and red, respectively. Proline residues are represented by black diamonds. (B) Regions that interact are colored green, whereas noninteracting regions are colored white.

sensitive reporters of the local backbone geometry and are routinely used in NMR studies of proteins as a measure of secondary structural propensities along the polypeptide chain. Figure 5A shows C^α and CO secondary chemical shifts measured in the free and Bin1-SH3-bound forms of NSSA(191–340). In addition, the SSP score³² that allows combination of all measured chemical shifts into a single value is plotted. A positive SSP score provides a quantitative measure of the percentage of conformers in the structural ensemble with α -helical geometry, while a negative SSP score indicates the percentage of extended local geometry. The SSP scores computed for free NSSA(191–340) are in good agreement with the previously reported results obtained for the longer NSSA(191–369) construct.¹⁷ From the SSP scores, we can identify three NSSA segments with α -helical propensities of approximately 40% for H1 (residues 205–221) and H2 (residues 251–266) and approximately 50% for H3 (residues 292–306). As expected, only the SSP scores in the two SH3 interaction regions, B1 and B2, comprising helical segments H1 and H3, respectively, were affected by Bin1-SH3 binding. Somewhat surprisingly, the population of α -helical structure decreases upon binding: the SSP scores in segment B1 are reduced to almost zero, while for B2, they are significantly

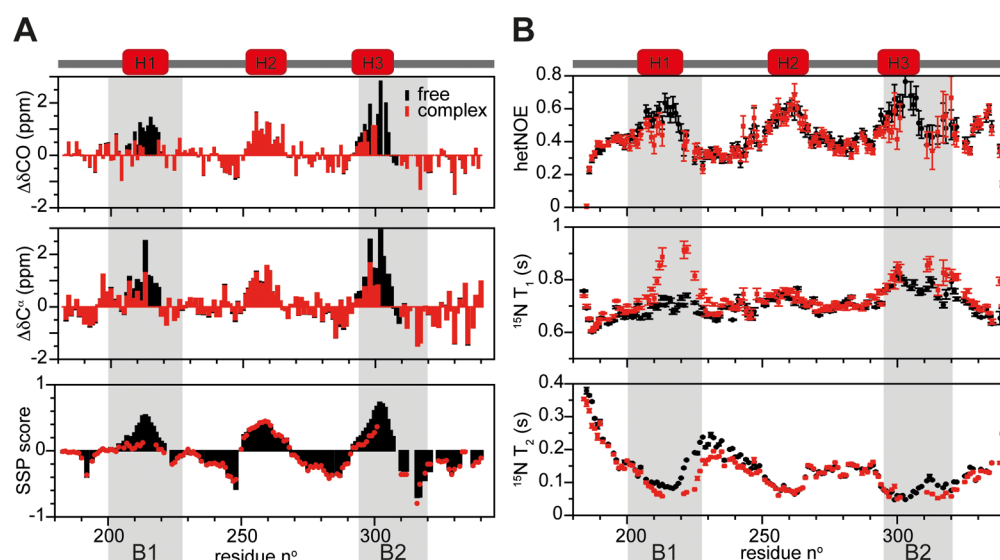


Figure 5. Structural and dynamical properties of NSSA(191–340) in its free (black) and Bin1-SH3-bound (red) states as derived from (A) CO and $\text{C}\alpha$ secondary chemical shifts and secondary structure propensities (SSP score) and (B) ^{15}N relaxation (T_1 , T_2 , and hetNOE). The regions that form transient α -helices H1–H3 are indicated at the top; the Bin1-SH3 binding regions are highlighted with gray bars.

reduced (although no ^{13}C chemical shifts could be measured for residues 214–217 and 302–309 because of extensive line broadening). The observed NMR parameters, i.e., chemical shifts, are population-weighted averages. Therefore, the differences observed between B1 and B2 might be due to the lower binding affinity of B2 resulting in a reduced population of NSSA molecules in complex with SH3 at the highest NSSA:SH3 molar ratio (1:10) that was used. For B1, more than 80% of the NSSA molecules are bound to SH3, while for B2, this number is reduced to 65%.

Complementary information about the conformational dynamics of NSSA in its free state and in complex with Bin1-SH3 was obtained from ^{15}N relaxation data (T_1 , T_2 , and hetNOE), plotted in Figure 5B as a function of NSSA sequence. Transiently populated helical segments H1, H2 and H3 are characterized by hetNOE values higher than those of the rest of the peptide chain, indicative of an increased level of local order, as well as a longer T_1 and a shorter T_2 , in agreement with an increase in the effective local tumbling correlation time, τ_c . As expected from the higher molecular weight of the complex, when SH3 binds tumbling correlation time τ_c is increased (longer T_1 and shorter T_2) in peptide regions B1 and B2 that bind to the SH3 domain. This observation most likely also explains the weak (or absent) NMR signals for the central residues in the binding site. More surprisingly, the hetNOE values of NSSA residues in the binding regions decrease upon interaction with SH3, in agreement with a more flexible structural ensemble. The interaction of NSSA with Bin1-SH3 via low-affinity binding sites B1 and B2 thus adds another example of a “fuzzy” complex^{34–36} formed between a globular protein domain and an intrinsically disordered protein (IDP).

DISCUSSION

Viruses extensively use the molecular machinery of the host cell for either their own replication or to interfere with the cellular defense mechanisms.³⁷ Nonstructural protein 5A of the hepatitis C virus is a prominent example for such a protein that has multiple functions during the viral life cycle and therefore needs to interact with a variety of viral and cellular

proteins.³⁸ NSSA belongs to the group of IDPs for which structural flexibility of the peptide chain presents a functional advantage in terms of binding promiscuity, as well as a high tolerance to mutations in the viral genome. Interactions are often mediated by short linear motifs that mimic binding sites of host proteins. A prominent example is the SH3 domain binding via PxxP motifs. Three such PxxP motifs are found in the low-complexity sequence LCS-2 of NSSA connecting domains 2 and 3.²⁰ Especially the second motif, PP2.2, was shown to interact with various SH3 domains.²¹ In this work, we used NMR spectroscopy to characterize these interactions at an atomic level.

Canonical SH3 Binding of NSSA Mediated by its PxxP Motifs (B3). The SH3 domains of the four selected proteins, Src, Fyn, PI3K, and Bin1, all interact with NSSA via the PP2.2 motif located in the LCS-2 region, although with different binding affinities. The strongest binder is the SH3 domain of Bin1 that has the most negatively charged binding groove (see Figure 1A). As the PP2.2 motif of NSSA is followed by three positively charged residues (R357, K358, and R359), the high affinity observed for Bin1-SH3 may be explained by additional electrostatic interactions in the binding pocket that are less efficient for the SH3 domains of kinases Src, Fyn, and PI3K.

Interestingly, some of our experimental results contradict previous reports in the literature. First, we observe binding of NSSA to Src-SH3, whereas no such interaction was detected in pull-down experiments.²¹ This discrepancy may be explained by the rather low affinity of NSSA for Src-SH3, and a large number of other SH3 domains present in the cell that compete for binding to NSSA. Second, the interaction of PI3K-SH3 with NSSA was reported previously to be independent of the PxxP motif in the LCS-2 region.^{39,40} However, while He et al.,³⁹ according to their pull-down experiments, suggest that the 110 N-terminal residues are necessary for interaction, Street et al.⁴⁰ conclude from their work on deletion mutants that the NSSA region of residues 270–300 is indispensable for SH3 binding. Our NMR results contradict both of these earlier findings, clearly demonstrating that under *in vitro* conditions PI3K-SH3 behaves very much like the other SH3 domains studied here, although we cannot completely rule out possible cross-talk

between binding regions B1 and B2 that is eliminated by the deletion of the intermediate fragment. In addition, under *in vivo* conditions where NSSA is attached to membranes and present in a dimeric state, cooperativity or cross-talk between the different binding sites might occur, which will influence the interaction modes. Finally, ITC measurements with Fyn-SH3 in complex with a short NSSA peptide containing the PP2.2 motif⁴¹ as well as SPR data for the complex of Fyn-SH3 with a NSSA D2-D3 construct⁴² are in agreement with a K_d in the submicromolar range, while our NMR observation of a fast exchange process between the free and bound form points toward a much lower binding affinity for this complex.

Noncanonical NSSA Binding to SH3 Domains Induces an Order-to-Disorder Transition. Here we have shown that NSSA interacts with SH3 domains via three distinct binding regions, with one (B3) corresponding to the canonical PxxP motif and the other two (B1 and B2) not containing such a canonical SH3 recognition element. Both of these additional binding sites are characterized by the presence of positively charged residues, similar to the positively charged segment in the C-terminal region of B3. These binding motifs, AKRRRL for B1 and LRKSRK for B2 (Figure 2C), are similar to the (R/K)xx(R/K) motif that has been reported to bind Gads-SH3^{5,6} and the (K/R)xxxxKx(K/R)(K/R) motif that also binds to the Bin1-SH3 domain.⁸ In addition, as reported by Kojima et al.,⁸ these positively charged peptide motifs interact with Bin1-SH3 through a surface region very similar to what is used for binding to PxxP motifs.

As noncanonical binding regions B1 and B2 correspond to a large extent to NSSA chain segments with a high propensity (40–50%) to exist in an α -helical conformation, we were also interested in structural changes induced by SH3 binding. Often, IDPs interact with their molecular targets via transiently populated secondary structural elements (α -helices or β -strands) that act as molecular recognition elements. Binding occurs via a conformational selection process in which the preformed structured conformation is stabilized in the complex, and the IDP undergoes an apparent disorder-to-order transition.^{43,44} However, it has also been reported that in some cases the IDP stays disordered even when it is bound to its target protein, forming a so-called fuzzy complex.^{34,35,45} One of these examples concerns NSSA, for which it has been reported³⁶ that domain 3 remains unstructured upon interaction with the major sperm protein (MSP) domain of VAPB forming a fuzzy complex. Here, in the case of the interaction of Bin1-SH3 with the noncanonical NSSA binding sites, we even observe an order-to-disorder transition, as the α -helical propensity and local order parameters (hetNOEs) are reduced upon complex formation. The fuzzy nature of the complex adds an entropic contribution to the binding free energy that otherwise seems to be governed by electrostatic interactions between the positively charged residues of NSSA in the binding region and the negatively charged interaction surface of Bin1-SH3. The fact that the transiently formed α -helices are not the recognition motifs for SH3 binding does not exclude the possibility that these preformed structural elements are of importance for interactions with other proteins. In that case, we may speculate that binding of NSSA to SH3 domains via these noncanonical binding sites inhibits binding to some other (still unknown) protein(s), thus contributing to the regulation of cellular processes by the virus.

At present, we can only speculate about the biological relevance of the different NSSA binding sites and modes of

binding to SH3 domains. Bin1 is known to form dimers *in vivo* through its BAR domain.⁴⁶ One may thus argue that such Bin1 dimers can form a very stable complex with a single NSSA molecule by simultaneously binding to the conventional PxxP motif and one of the noncanonical binding regions. This may allow translocation of Bin1 even at low cellular NSSA concentrations. It has also been shown that the interaction of Bin1 with NSSA inhibits its phosphorylation, although the exact molecular mechanisms remain unknown.¹² A possible role of binding of Bin1-SH3 to the noncanonical binding regions in NSSA is therefore the inhibition of phosphorylation by preventing kinases from accessing the phosphorylation sites.

In conclusion, we have characterized the interaction of viral protein NSSA with SH3 domains of several kinases and tumor suppressor Bin1. Besides the well-known PxxP motif interacting with the SH3 domain, we were able to identify two additional binding regions in NSSA that bind at an SH3 surface location similar to that of the PxxP motif, mainly through electrostatic interactions. Surprisingly, the transiently formed α -helices that are present in the binding regions of free NSSA are destabilized in the NSSA-SH3 complex. These additional SH3 binding modes may be important for the regulation of molecular interaction and phosphorylation events that NSSA undergoes during the viral life cycle.

■ ASSOCIATED CONTENT

● Supporting Information

An overlay of 2D BEST-TROSY spectra of NSSA(191–340) and NSSA(191–369) (Figure S1) and measured chemical shift changes for Bin1-SH3 in the presence of either the B1(200–228) or the B2(295–320) peptide (Figure S2). This material is available free of charge via the Internet at <http://pubs.acs.org>.

■ AUTHOR INFORMATION

Corresponding Author

*Biomolecular NMR Spectroscopy group, Institut de Biologie Structurale, Jean Pierre Ebel 41, rue Jules Horowitz, 38027 Grenoble Cedex 1, France. E-mail: bernhard.brutscher@ibs.fr. Phone: +33 4 38 78 95 62. Fax: +33 4 38 78 54 94.

Funding

This work has been supported by grants from the European Commission (FP7-ITN IDPbyNMR Contract 264257) and the Deutsche Forschungsgemeinschaft (SFB974, A11).

Notes

The authors declare no competing financial interest.

■ ACKNOWLEDGMENTS

We thank Adrian Favier and Isabel Ayala for technical support and help with protein expression and Enrico Rennella for the fitting of the titration curves.

■ ABBREVIATIONS

BEST, band-selective excitation short transient; Bin1, bridging integrator protein 1; DDEF1, development- and differentiation-enhancing factor 1; HCV, hepatitis C virus; hetNOE, heteronuclear $\{^1\text{H}\}$ – ^{15}N nuclear Overhauser enhancement; IDP, intrinsically disordered protein; LCS, low-complexity sequence; NSSA, nonstructural protein 5A; PDB, Protein Data Bank; PPII, polyproline type II; SH3, Src homology 3; TROSY, transverse relaxation-optimized spectroscopy.

REFERENCES

- (1) Musacchio, A. (2002) How SH3 domains recognize proline. *Adv. Protein Chem.* 61, 211–268.
- (2) Saksela, K., and Permi, P. (2012) SH3 domain ligand binding: What's the consensus and where's the specificity? *FEBS Lett.* 586, 2609–2614.
- (3) Kaieda, S., Matsui, C., Mimori-Kiyosue, Y., and Ikegami, T. (2010) Structural basis of the recognition of the SAMP motif of adenomatous polyposis coli by the Src-homology 3 domain. *Biochemistry* 49, 5143–5153.
- (4) Aitio, O., Hellman, M., Kesti, T., Kleino, I., Samuilova, O., Paakkonen, K., Tossavainen, H., Saksela, K., and Permi, P. (2008) Structural basis of PxxDY motif recognition in SH3 binding. *J. Mol. Biol.* 382, 167–178.
- (5) Berry, D. M., Nash, P., Liu, S. K., Pawson, T., and McGlade, C. J. (2002) A high-affinity Arg-X-X-Lys SH3 binding motif confers specificity for the interaction between Gads and SLP-76 in T cell signaling. *Curr. Biol.* 12, 1336–1341.
- (6) Liu, Q., Berry, D., Nash, P., Pawson, T., McGlade, C. J., and Li, S. S. (2003) Structural basis for specific binding of the Gads SH3 domain to an RxxK motif-containing SLP-76 peptide: A novel mode of peptide recognition. *Mol. Cell* 11, 471–481.
- (7) Perez, Y., Maffei, M., Igea, A., Amata, I., Gairi, M., Nebreda, A. R., Bernado, P., and Pons, M. (2013) Lipid binding by the Unique and SH3 domains of c-Src suggests a new regulatory mechanism. *Sci. Rep.* 3, 1295.
- (8) Kojima, C., Hashimoto, A., Yabuta, I., Hirose, M., Hashimoto, S., Kanaho, Y., Sumimoto, H., Ikegami, T., and Sabe, H. (2004) Regulation of Bin1 SH3 domain binding by phosphoinositides. *EMBO J.* 23, 4413–4422.
- (9) Nicot, A. S., Toussaint, A., Tosch, V., Kretz, C., Wallgren-Pettersson, C., Iwarsson, E., Kingston, H., Garnier, J. M., Biancalana, V., Oldfors, A., Mandel, J. L., and Laporte, J. (2007) Mutations in amphiphysin 2 (BIN1) disrupt interaction with dynamin 2 and cause autosomal recessive centronuclear myopathy. *Nat. Genet.* 39, 1134–1139.
- (10) Sakamuro, D., Elliott, K. J., Wechsler-Reya, R., and Prendergast, G. C. (1996) BIN1 is a novel MYC-interacting protein with features of a tumour suppressor. *Nat. Genet.* 14, 69–77.
- (11) Neuvonen, M., Kazlauskas, A., Martikainen, M., Hinkkanen, A., Ahola, T., and Saksela, K. (2011) SH3 domain-mediated recruitment of host cell amphiphysins by alphavirus nsP3 promotes viral RNA replication. *PLoS Pathog.* 7, e1002383.
- (12) Masumi, A., Aizaki, H., Suzuki, T., DuHadaway, J. B., Prendergast, G. C., Komuro, K., and Fukazawa, H. (2005) Reduction of hepatitis C virus NSSA phosphorylation through its interaction with amphiphysin II. *Biochem. Biophys. Res. Commun.* 336, 572–578.
- (13) Nanda, S. K., Herion, D., and Liang, T. J. (2006) The SH3 binding motif of HCV NSSA protein interacts with Bin1 and is important for apoptosis and infectivity. *Gastroenterology* 130, 794–809.
- (14) Zech, B., Kurtenbach, A., Krieger, N., Strand, D., Blencke, S., Morbitzer, M., Salassidis, K., Cotten, M., Wissing, J., Obert, S., Bartenschlager, R., Herget, T., and Daub, H. (2003) Identification and characterization of amphiphysin II as a novel cellular interaction partner of the hepatitis C virus NSSA protein. *J. Gen. Virol.* 84, 555–560.
- (15) Tellinghuisen, T. L., Marcotrigiano, J., Gorbalenya, A. E., and Rice, C. M. (2004) The NSSA protein of hepatitis C virus is a zinc metalloprotein. *J. Biol. Chem.* 279, 48576–48587.
- (16) Brass, V., Bieck, E., Montserret, R., Wolk, B., Hellings, J. A., Blum, H. E., Penin, F., and Moradpour, D. (2002) An amino-terminal amphipathic α -helix mediates membrane association of the hepatitis C virus nonstructural protein 5A. *J. Biol. Chem.* 277, 8130–8139.
- (17) Feuerstein, S., Solyom, Z., Aladag, A., Favier, A., Schwarten, M., Hoffmann, S., Willbold, D., and Brutscher, B. (2012) Transient structure and SH3 interaction sites in an intrinsically disordered fragment of the hepatitis C virus protein NSSA. *J. Mol. Biol.* 420, 310–323.
- (18) Hanouille, X., Badillo, A., Verdegem, D., Penin, F., and Lippens, G. (2010) The domain 2 of the HCV NSSA protein is intrinsically unstructured. *Protein Pept. Lett.* 17, 1012–1018.
- (19) Hanouille, X., Verdegem, D., Badillo, A., Wieruszkeski, J. M., Penin, F., and Lippens, G. (2009) Domain 3 of non-structural protein 5A from hepatitis C virus is natively unfolded. *Biochem. Biophys. Res. Commun.* 381, 634–638.
- (20) Tan, S. L., Nakao, H., He, Y., Vijaysri, S., Neddermann, P., Jacobs, B. L., Mayer, B. J., and Katze, M. G. (1999) NSSA, a nonstructural protein of hepatitis C virus, binds growth factor receptor-bound protein 2 adaptor protein in a Src homology 3 domain/ligand-dependent manner and perturbs mitogenic signaling. *Proc. Natl. Acad. Sci. U.S.A.* 96, 5533–5538.
- (21) Macdonald, A., Crowder, K., Street, A., McCormick, C., and Harris, M. (2004) The hepatitis C virus NSSA protein binds to members of the Src family of tyrosine kinases and regulates kinase activity. *J. Gen. Virol.* 85, 721–729.
- (22) Feuerstein, S., Solyom, Z., Aladag, A., Hoffmann, S., Willbold, D., and Brutscher, B. (2011) ^1H , ^{13}C , and ^{15}N resonance assignment of a 179 residue fragment of hepatitis C virus non-structural protein 5A. *Biomol. NMR Assignments* 5, 241–243.
- (23) Batra-Safferling, R., Granzin, J., Modder, S., Hoffmann, S., and Willbold, D. (2010) Structural studies of the phosphatidylinositol 3-kinase (PI3K) SH3 domain in complex with a peptide ligand: Role of the anchor residue in ligand binding. *Biol. Chem.* 391, 33–42.
- (24) Schmidt, H., Hoffmann, S., Tran, T., Stoldt, M., Stangler, T., Wiesehan, K., and Willbold, D. (2007) Solution structure of a Hck SH3 domain ligand complex reveals novel interaction modes. *J. Mol. Biol.* 365, 1517–1532.
- (25) Tran, T., Hoffmann, S., Wiesehan, K., Jonas, E., Luge, C., Aladag, A., and Willbold, D. (2005) Insights into human Lck SH3 domain binding specificity: Different binding modes of artificial and native ligands. *Biochemistry* 44, 15042–15052.
- (26) Delaglio, F., Grzesiek, S., Vuister, G. W., Zhu, G., Pfeifer, J., and Bax, A. (1995) NMRPipe: A multidimensional spectral processing system based on UNIX pipes. *J. Biomol. NMR* 6, 277–293.
- (27) Vranken, W. F., Boucher, W., Stevens, T. J., Fogh, R. H., Pajon, A., Llinas, M., Ulrich, E. L., Markley, J. L., Ionides, J., and Laue, E. D. (2005) The CCPN data model for NMR spectroscopy: Development of a software pipeline. *Proteins* 59, 687–696.
- (28) Favier, A., and Brutscher, B. (2011) Recovering lost magnetization: Polarization enhancement in biomolecular NMR. *J. Biomol. NMR* 49, 9–15.
- (29) Solyom, Z., Schwarten, M., Geist, L., Konrat, R., Willbold, D., and Brutscher, B. (2013) BEST-TROSY experiments for time-efficient sequential resonance assignment of large disordered proteins. *J. Biomol. NMR* 55, 311–321.
- (30) Schwarzwinger, S., Kroon, G. J., Foss, T. R., Chung, J., Wright, P. E., and Dyson, H. J. (2001) Sequence-dependent correction of random coil NMR chemical shifts. *J. Am. Chem. Soc.* 123, 2970–2978.
- (31) Zhang, H., Neal, S., and Wishart, D. S. (2003) RefDB: A database of uniformly referenced protein chemical shifts. *J. Biomol. NMR* 25, 173–195.
- (32) Marsh, J. A., Singh, V. K., Jia, Z., and Forman-Kay, J. D. (2006) Sensitivity of secondary structure propensities to sequence differences between α - and γ -synuclein: Implications for fibrillation. *Protein Sci.* 15, 2795–2804.
- (33) Farrow, N. A., Muhandiram, R., Singer, A. U., Pascal, S. M., Kay, C. M., Gish, G., Shoelson, S. E., Pawson, T., Forman-Kay, J. D., and Kay, L. E. (1994) Backbone dynamics of a free and phosphopeptide-complexed Src homology 2 domain studied by ^{15}N NMR relaxation. *Biochemistry* 33, 5984–6003.
- (34) Fuxreiter, M. (2012) Fuzziness: Linking regulation to protein dynamics. *Mol. Biosyst.* 8, 168–177.
- (35) Fuxreiter, M., and Tompa, P. (2012) Fuzzy complexes: A more stochastic view of protein function. *Adv. Exp. Med. Biol.* 725, 1–14.
- (36) Gupta, G., Qin, H., and Song, J. (2012) Intrinsically unstructured domain 3 of hepatitis C Virus NSSA forms a “fuzzy

complex" with VAPB-MSP domain which carries ALS-causing mutations. *PLoS One* 7, e39261.

(37) Davey, N. E., Trave, G., and Gibson, T. J. (2011) How viruses hijack cell regulation. *Trends Biochem. Sci.* 36, 159–169.

(38) Bode, J. G., Brenndorfer, E. D., Karthe, J., and Haussinger, D. (2009) Interplay between host cell and hepatitis C virus in regulating viral replication. *Biol. Chem.* 390, 1013–1032.

(39) He, Y., Nakao, H., Tan, S. L., Polyak, S. J., Neddermann, P., Vijaysri, S., Jacobs, B. L., and Katze, M. G. (2002) Subversion of cell signaling pathways by hepatitis C virus nonstructural 5A protein via interaction with Grb2 and P85 phosphatidylinositol 3-kinase. *J. Virol.* 76, 9207–9217.

(40) Street, A., Macdonald, A., Crowder, K., and Harris, M. (2004) The hepatitis C virus NS5A protein activates a phosphoinositide 3-kinase-dependent survival signaling cascade. *J. Biol. Chem.* 279, 12232–12241.

(41) Martin-Garcia, J. M., Luque, I., Ruiz-Sanz, J., and Camara-Artigas, A. (2012) The promiscuous binding of the Fyn SH3 domain to a peptide from the NS5A protein. *Acta Crystallogr. D* 68, 1030–1040.

(42) Shelton, H., and Harris, M. (2008) Hepatitis C virus NS5A protein binds the SH3 domain of the Fyn tyrosine kinase with high affinity: Mutagenic analysis of residues within the SH3 domain that contribute to the interaction. *Virol. J.* 5, 24.

(43) Sugase, K., Dyson, H. J., and Wright, P. E. (2007) Mechanism of coupled folding and binding of an intrinsically disordered protein. *Nature* 447, 1021–1025.

(44) Wright, P. E., and Dyson, H. J. (2009) Linking folding and binding. *Curr. Opin. Struct. Biol.* 19, 31–38.

(45) Mittag, T., Kay, L. E., and Forman-Kay, J. D. (2010) Protein dynamics and conformational disorder in molecular recognition. *J. Mol. Recognit.* 23, 105–116.

(46) Casal, E., Federici, L., Zhang, W., Fernandez-Recio, J., Priego, E. M., Miguel, R. N., DuHadaway, J. B., Prendergast, G. C., Luisi, B. F., and Laue, E. D. (2006) The crystal structure of the BAR domain from human Bin1/amphiphysin II and its implications for molecular recognition. *Biochemistry* 45, 12917–12928.

(47) Baker, N. A., Sept, D., Joseph, S., Holst, M. J., and McCammon, J. A. (2001) Electrostatics of nanosystems: Application to microtubules and the ribosome. *Proc. Natl. Acad. Sci. U.S.A.* 98, 10037–10041.

(48) *The PyMOL Molecular Graphics System* (2010) Schrodinger, LLC.